

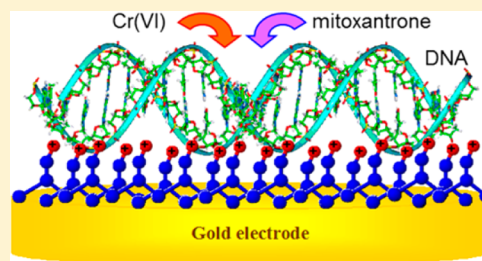
Chromium(VI) but Not Chromium(III) Species Decrease Mitoxantrone Affinity to DNA

Anna M. Nowicka,^{†,§} Zbigniew Stojek,[‡] and Maria Hepel^{*,†}

[†]Department of Chemistry, State University of New York at Potsdam, Potsdam, New York 13676, United States

[‡]Department of Chemistry, University of Warsaw, PL-02093 Warsaw, Poland

ABSTRACT: Binding of mitoxantrone (MXT) to double-stranded DNA has been investigated as a model drug–DNA binding system to evaluate the effects of various forms of chromium on the binding properties. We have found that Cr(III), which binds strongly to DNA, does not affect the MXT affinity to DNA. In contrast, Cr(VI), in the form of chromate ions CrO_4^{2-} , decreases the MXT affinity to DNA despite electrostatic repulsions with phosphate–deoxyribose chains of DNA. The MXT–DNA binding constant was found to decrease from $(1.96 \pm 0.005) \times 10^5$ to $(0.77 \pm 0.018) \times 10^5 \text{ M}^{-1}$ for Cr(VI) concentration changing from 0 to 30 μM . The influence of Cr(VI) on MXT–DNA binding has been attributed to the oxidation of guanine residue, thus interrupting the intercalation of MXT into the DNA double helix at the preferential CpG intercalation site. This supposition is corroborated by the observed increase in the MXT binding site size from 2 bp (base pairs) to 4–6 bp in the presence of Cr(VI). The measurements of the MXT–DNA binding constant and the MXT binding site size on a DNA molecule have been carried out using spectroscopic, voltammetric, and nanogravimetric techniques, providing useful information on the mechanism of the interactions.



1. INTRODUCTION

The interactions of chromium species with DNA have been extensively investigated due to the mutagenicity of Cr(VI) and its considerable threat to human health.¹ Cr(III) is generally considered as an essential and nontoxic supplement necessary for human health;^{2,3} however, some studies have shown that, under certain conditions, Cr(III) can cause significant damage to DNA.⁴ Our measurements indicate that, in addition to the mutagenic properties of Cr(VI), it may also act to decrease the affinity of biomolecules and drugs to DNA despite the strong mutual electrostatic repulsions between CrO_4^{2-} and negatively charged deoxyribose–phosphate chains of DNA. In this work, we have investigated the effect of Cr(VI) and other chromium species on the binding properties of a model drug mitoxantrone (MXT) to double-stranded DNA (dsDNA) immobilized on a gold piezoresonator surface which enabled direct observations and new physical insights into the drug binding and release properties. The influence of Cr(VI) on MXT binding to DNA is contrasted with the effect of Cr(III), for which we have found strong association with DNA but no influence on binding of MXT to DNA.

The MXT–DNA system represents a model drug–DNA binding system. It has been thoroughly investigated due to its clinical significance, as the MXT–DNA binding plays the key role in MXT-based chemotherapy of several cancers, including breast malignancies,^{5–7} ovarian cancer, and several leukemias.⁸ Widespread interest in MXT can be attributed to its high potency and lower cardiotoxicity as compared to the competing drugs: anthracycline, doxorubicin, and daunorubicin. Whereas the mechanism of action of MXT is not completely understood,

it is commonly assumed that MXT binds to DNA by intercalation.^{9,10} The intercalation binding occurs preferentially at the CpG base sequence, with side chains of MXT lying in the minor groove of DNA.^{11,12} It is also known that the intercalation of MXT with the DNA double helix interferes with the strand reunion reaction of topoisomerase II and results in the production of protein-linked DNA double-strand breaks.^{13–15} The production of reactive oxygen species (ROS) has been considered to be a major cytotoxic effect of MXT on cancer cells.¹⁶ However, the significance of DNA condensation caused by the intercalation of MXT is far reaching,¹⁷ as it inhibits DNA replication and RNA transcription, thus contributing to tumor destruction.^{10,14}

The interactions of MXT with DNA have been examined by various biochemical and physicochemical methods including DNA foot printing assay,¹⁸ molecular dynamics simulation,¹² electrical linear dichroism,¹⁹ scanning electron microscopy,⁹ spectroscopy,²⁰ and electrochemistry.^{21–28} In this work, we have investigated the interactions of MXT with DNA in solution as well as with DNA immobilized on a piezoresonator surface which can serve as a versatile and very sensitive platform for DNA studies,^{29–38} complementing those carried out by voltammetric techniques.^{39–52}

On the other hand, various chromium species have a contrasting impact on the environment and health.⁵³ Trivalent chromium, Cr(III), is required in trace amounts for sugar and

Received: November 5, 2012

Revised: December 26, 2012

Published: January 7, 2013

lipid metabolism in humans, and the depletion of Cr(III) may lead to a chromium deficiency disease⁵⁴ (the adequate daily dietary intake of Cr(III) for adults is 50–200 $\mu\text{g}/\text{d}^2$). In contrast, hexavalent chromium, Cr(VI), is very toxic and mutagenic^{1,55–58} and causes lung cancer when inhaled.^{58,59}

The use of chromium-containing dietary supplements is controversial due to the complex effects of the supplements used.^{60,61} For instance, the popular supplement, chromium picolinate complex, generates chromosome damage in hamster cells.⁶² Several in vitro studies have indicated that high concentrations of chromium(III) in cells can lead to DNA damage.³ Acute oral toxicity ranges between 1500 and 3300 $\mu\text{g}/\text{kg}$.⁶¹ The proposed beneficial effects of Cr(III) and the use as dietary supplements yielded some controversial results, but recent reviews suggest that moderate uptake of chromium(III) through dietary supplements poses no risk.³

The maximum allowable concentration in drinking water for Cr(VI), recommended by the World Health Organization, is 50 $\mu\text{g}/\text{L}$. Hexavalent chromium is restricted by the European Restriction of Hazardous Substances Directive. The acute oral toxicity for Cr(VI) ranges between 50 and 150 $\mu\text{g}/\text{kg}$.⁶¹ In the body, most of the Cr(VI) is reduced by several mechanisms to Cr(III), already in the blood before it enters the cells. The Cr(III) is excreted from the body, whereas the chromate ion is transferred to the cells by anion transport mechanism.

The acute toxicity of Cr(VI) is due to its strong oxidative properties. After it reaches the bloodstream, it damages the kidneys, liver, and blood cells through various oxidation reactions. The hemolysis as well as the renal and liver failures are the results of these damages. Aggressive dialysis can improve the prognosis.⁶³

The mechanisms of interactions of Cr(III) and Cr(VI) with DNA have been investigated by Arakawa et al.⁶⁴ using UV–vis and FTIR techniques. According to the authors, Cr(III) binds to guanine N-7 and the nearest PO_2 group, forming a chelate with binding constant $K = 3.15 \times 10^3 \text{ M}^{-1}$. At very high concentrations of Cr(III), the DNA condensation takes place.⁶⁴ The interactions of Cr(VI) with DNA have been found to be much weaker ($K = 508 \text{ M}^{-1}$) and most likely involve reductive association rather than direct binding of Cr(VI) species.⁶⁴ In the first step of DNA oxidation by Cr(VI), the guanine residue is oxidized to 7,8-dihydro-8-oxoguanine (oxoG) which is a major premutagenic lesion.^{64,65}

So far, no report has been published on the effect of chromium species on MXT–DNA binding. Our preliminary experiments have indicated that Cr(VI) influences the MXT affinity to DNA while Cr(III) does not. This result is in clear disagreement with the propensity of Cr(III) to associate with DNA and mutual repulsions between CrO_4^{2-} and phosphate–deoxyribose chains of DNA. Therefore, in this work, detailed investigations of the voltammetric, nanogravimetric, and spectroscopic characteristics of MXT binding to DNA in the presence of Cr(VI) and Cr(III) have been carried out. The changes in MXT binding site size in the DNA matrix have also been monitored. The fluorescence emission spectra were also obtained to determine the mode of these interactions.

2. METHODS

Chemicals. Mitoxantrone (MXT) (1,4-dihydroxy-5,8-bis[2-(2-hydroxyethylamino)ethylamino]-anthracene-9,10-dione) was obtained from Sigma Aldrich Chemical Co. (Atlanta, GA). The MXT stock solution of 1 mM was prepared once a week and was screened from light to avoid photochemical

decomposition. The stock solution was diluted just before use. Calf thymus double-stranded DNA (dsDNA) was purchased from Sigma Aldrich. The dsDNA purity was tested by measuring the absorbance A at $\lambda = 250, 260$, and 280 nm . Only the samples showing the ratios $A_{260}/A_{280} = 1.7\text{--}2.0$ and $A_{260}/A_{250} = 1.4\text{--}1.7$ were used for measurements. The dsDNA solutions of 1 mg of DNA per 1 mL of PBS buffer (pH 7.4) were prepared at least 24 h before experiments. The dsDNA concentration was determined on the basis of the absorbance at $\lambda = 260 \text{ nm}$; $\epsilon = 13\,200 \text{ M}^{-1} \text{ cm}^{-1}$.⁶⁶ The Cr(VI) source was K_2CrO_4 , and the Cr(III) source was $\text{Cr}(\text{NO}_3)_3 \cdot 9\text{H}_2\text{O}$. Ascorbic acid (AA) was obtained from Sigma Aldrich. The pK_a of ascorbic acid is 4.2; thus, in 0.02 M PBS buffer (pH 7.4), AA exists as the monoanion ascorbate. Poly(allylamine hydrochloride) (PAH) was purchased from Fisher Scientific (Pittsburgh, PA). The pK_a of PAH is 8.5; thus, in 0.02 M PBS buffer (pH 7.4), it exists predominantly as a polycation.

Fluorimetric Titration. Fluorescence experiments were carried out with a PerkinElmer LS 55 fluorescence spectrometer. A quartz cuvette of 1 cm was used. The fluorescence titrations were performed by keeping the constant concentration of the drug (MXT) while varying the concentration of DNA. Continuous stirring was made throughout the course of the titration. The spectra were recorded 1 h after preparing the solutions.

Electrochemical Measurements. Linear scan voltammetry (LSV) studies were performed with an Elchemia Model PS-1705 potentiostat. All voltammetric experiments were carried out in a three-electrode system. A platinum wire served as the counter electrode, a Ag/AgCl electrode was used as the reference electrode, and a 3 mm diameter glassy carbon disc electrode (GC) was employed as the working electrode. The GC electrode was polished before each measurement with 0.3 and, at the end, 0.05 μm Al_2O_3 powders on a wet pad. After polishing, the alumina oxide was removed by rinsing the electrode surface with a direct stream of ultrapure water (Milli-Q, Milipore, Billerica, MA; conductivity: 0.056 $\mu\text{S}/\text{cm}$). During the voltammetric experiments, the electrochemical cell was kept in a Faraday cage to minimize the electrical noise. Before experiments, all analyzed solutions were deoxygenated with pure argon for 15 min.

Nanogravimetric Measurements. An electrochemical quartz crystal nanobalance model EQCN-700 (Elchemia, Potsdam, NY) with 10 MHz AT-cut quartz crystal resonators was used in this study. The EQCN technique allowed simultaneous monitoring of voltammetric and nanogravimetric curves. The resonant frequency of the quartz crystal lattice vibrations in a thin quartz crystal wafer was measured as a function of the mass attached to the crystal interfaces. For thin rigid films, the interfacial mass changes Δm are related to the shift in the series resonance oscillation frequency Δf of the EQCN through the Sauerbrey equation:^{29,67}

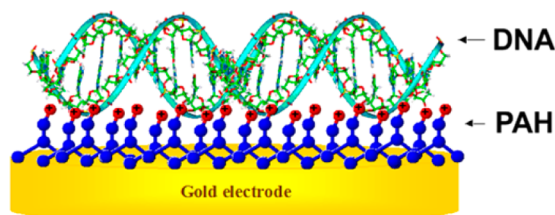
$$\Delta f = \frac{2\Delta m n f_0^2}{A \sqrt{\mu_q \rho_q}} \quad (1)$$

where f_0 is the oscillation frequency in the fundamental mode, n is the overtone number, A is the piezoelectrically active surface area, ρ_q is the density of quartz ($\rho_q = 2.648 \text{ g cm}^{-3}$), and μ_q is the shear modulus of quartz ($\mu_q = 2.947 \times 10^{11} \text{ g cm}^{-1} \text{ s}^{-2}$). The oscillator was tuned to the series resonance frequency of working piezoelectrodes to minimize effects due to energy dissipation in protein films. All experimental variables

influencing the resonant frequency²⁹ of the EQCN electrodes such as the temperature, pressure, viscosity, and density of the solution were kept constant to prevent frequency variation due to the changes of these parameters. The piezoelectrically active (geometrical) surface area of the working Au electrode was 0.196 cm² and the real surface area $A = 0.255$ cm² (roughness factor $R = 1.3$). A 200 nm thick Au film was deposited on a 14 mm diameter, 0.166 mm thick, AT-cut quartz resonator wafer with a vacuum deposited Ti adhesion interlayer (20 nm thick). The real surface area of the Au-EQCN electrodes was determined by the standard monolayer oxide formation procedure.⁶⁸ The resonator crystals were sealed to the side opening in a glass vessel of a 50 mL capacity using high purity siloxane glue with intermediate viscosity (Elchema SS-431). The seal was cured for 24 h at room temperature. The working electrode was polarized using a Pt wire counter electrode, and its potential was measured versus a double-junction saturated Ag/AgCl electrode.

Immobilization of DNA in a Polymeric Film. The Au-EQCN electrode surface was cleaned by cycling in 0.1 M H₂SO₄ in the potential range 0–1.5 V until a stable voltammogram was recorded. This was followed by immersing the electrode in a piranha etching solution (30% H₂O₂:H₂SO₄ = 1:3) for 10 s and rinsing it with distilled water. The Au/PAH (poly(allylamine hydrochloride)) films were formed by soaking a QC/Au piezoelectrode in 30 mL of a 3 mg/mL PAH solution in 0.5 M NaCl (pH 5). A 3 mg/mL PAH aqueous solution contained polycations. By applying a potential of –50 mV for 1 h, a PAH film was formed on a gold electrode surface. Then, the electrode and the cell were delicately rinsed with distilled water. DNA was adsorbed from a 0.02 M PBS buffer (pH 7.4) containing dsDNA (100 μM base pairs) by applying the potential of +50 mV for 1 h. Finally, such a modified electrode was ready for studying DNA interactions with MXT. The design of a Au/PAH/DNA modified electrode is depicted in Scheme 1. The amount of DNA adsorbed at the PAH layer was

Scheme 1. Scheme of Preparation of a PAH/DNA-Modified Gold-Coated Piezoelectrode for EQCN Measurements



determined from the differences of the absorbance of DNA solution at 260 nm before and after the immobilization process. In all cases, this value was approximately 2 μM base pairs.

Data Analysis. The binding parameters of the drug–DNA interactions were determined in 0.02 M PBS buffer of pH 7.4. A useful tool to determine these parameters, regardless of the technique used, is the polymer model of McGhee and von Hippel.⁶⁹ The following formula describes the interactions between the dsDNA strand and the ligand:

$$\frac{r}{C_f} = K(1 - nr) \left[\frac{1 - nr}{1 - (n - 1)r} \right]^{n-1} \quad (2)$$

where K is the binding constant, n is the number of binding matrix units that are occupied by one molecule of the drug, and

$r = C_b/C_{m.u.}$, where $C_b = C_0 - C_f$, C_b is the concentration of the ligand molecules bound to dsDNA, C_0 is the total concentration of the ligand, C_f is the concentration of the free molecules of the ligand in the solution, and $C_{m.u.}$ is the analytical concentration of the binding units in dsDNA. The assumptions of the model fit the experimental reality very well. The lattice is assumed to be homogeneous, is taken as a linear array of many repeating units, and the basic lattice residue corresponds to a nucleic acid base-pair. A ligand molecule is assumed to bind to the lattice and to cover n consecutive lattice residues. The occupied residue is inaccessible to another ligand. To determine K and n , the concentrations of unbound and bound drug should be known. If so, then the Scatchard plot ($r/C_f = f(r)$) can be constructed. The extraction of K and n values is done by numeric fitting of the experimental data to eq 2. Concentrations of free MXT (C_f) were determined by subtracting the masses of complexed MXT from the total drug used for the experiment. The values of the complexed drug mass were taken from the EQCN measurements. Concentrations of the binding unit in dsDNA immobilized at the PAH layer ($C_{m.u.}$) and concentrations of the MXT molecules bound to dsDNA (C_b) were determined from the mass increases at the electrode active surface area. C_b and $C_{m.u.}$ are surface concentrations and therefore are given in g cm^{–2}, while C_f is in mol/L. In consequence, the unit of K is determined by C_f .

3. RESULTS AND DISCUSSION

Interaction of MXT with DNA. The cyclic voltammograms obtained in a 0.01 M PBS buffer (pH 7.4) show that the oxidation of MXT at the glassy carbon electrode is an irreversible process. Typical CV curves are presented in Figure 1a. The first oxidation peak that appears at 0.35 V corresponds to the oxidation of the hydroxyl groups at positions 5 and 8. The second peak, at 0.51 V, corresponds to the oxidation of the aminoalkyl substituents after tautomeric structural rearrangements. Each of the steps involves a two-electron transfer.^{21,70} MXT in the PBS buffer of pH 7.4 exists as a dication (Scheme 2), so the attractions between the negatively charged DNA strands and positively charged MXT molecules should be observed.

In the presence of DNA in solution, both anodic peaks of MXT vanish (Figure 1b). It means that there are nearly no free MXT in the solution. Additionally, the intensity of the oxidation current of guanine at 0.75 mV increases with additions of the drug to the solution; the peaks are seen well after background subtraction. This suggests that the intercalation of MXT does not lead to the loss of the electrochemical activity of the guanine molecules. Since the electrochemical signals of the drug and DNA are well separated, the concentration of a free drug can be determined from the changes of the drug current.

The investigation of the MXT interactions with dsDNA was also carried out using polished Au–EQCN electrodes modified with PAH/DNA. The binding of ca. 330 ng to the electrode was observed upon addition of MXT to the solution (0.6 μM); see Figure 1B. The constructed Scatchard plots from LSV and EQCN results are presented in Figure 2. The mean values of the binding parameters: binding constant (K) and the binding-site size (n) obtained by fitting eq 2 to the experimental data are 2.32×10^5 M^{–1} and 2.17, respectively. These values are consistent with those reported for the interaction of anthracycline molecules with DNA ($K = 10^4$ – 10^5 M^{–1}).⁷¹

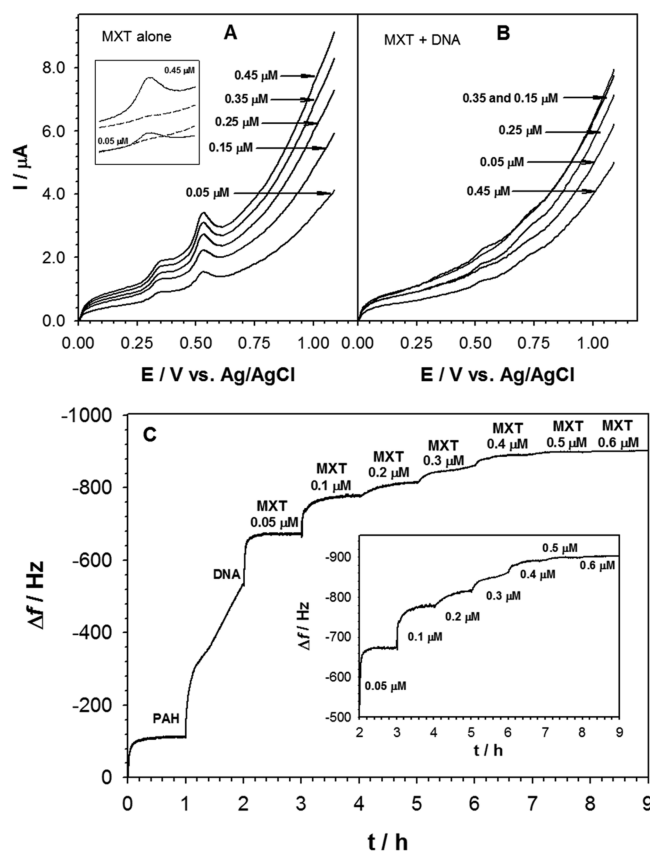
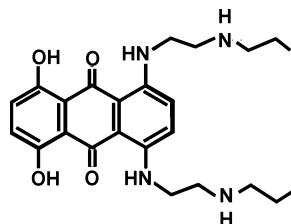


Figure 1. (A, B) Linear scan voltammograms of MXT obtained in the absence (A) and presence (B) of dsDNA, for C_{MXT} from 50 to 3450 nM. Experimental conditions: $t = 23\text{ }^{\circ}\text{C}$; $\phi_{\text{GC}} = 3\text{ mm}$; $C_{\text{DNA}} = 2.6\text{ }\mu\text{M}$ bp (base pairs), $\nu = 100\text{ mV/s}$; voltammograms were obtained 1 h after solution preparation. Inset in A: an enlargement of the second peak, around 0.5 V. (C) EQCN frequency shifts upon each step of electrode surface modification; buffer: 0.02 M PBS, pH 7.4.

Scheme 2. Structure of Mitoxantrone in PBS Buffer (pH 7.4)



The Scatchard plots are linear, indicating that only one type of interactions occurs.

Interaction of MXT with DNA in the Presence of Cr(VI). For this study, two approaches have been used. In the first one, the Au/PAH/DNA modified electrode was immersed in a sequence of solutions containing various MXT concentrations and a constant Cr(VI) concentration ($5\text{ }\mu\text{M}$). Typical plots of the frequency shifts after each MXT addition and the corresponding current changes are presented in Figure 3. The values determined for the binding constant and the binding site size are $2.02 \times 10^5\text{ M}^{-1}$ and 2.23 (the mean values from LSV and EQCN), respectively. The values of the binding parameters obtained in the presence of Cr(VI) from the LSV and EQCN results do not differ significantly compared to those determined in the absence of Cr(VI) in the solution. Only in the case of a significant excess of Cr(VI) (7 times or higher

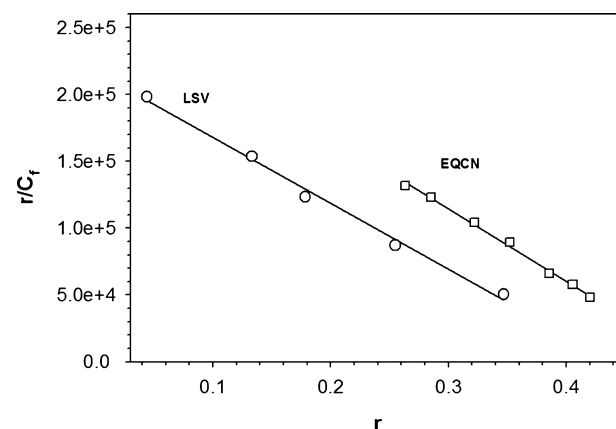


Figure 2. Scatchard plots for binding of MXT to dsDNA obtained from LSV and EQCN results.

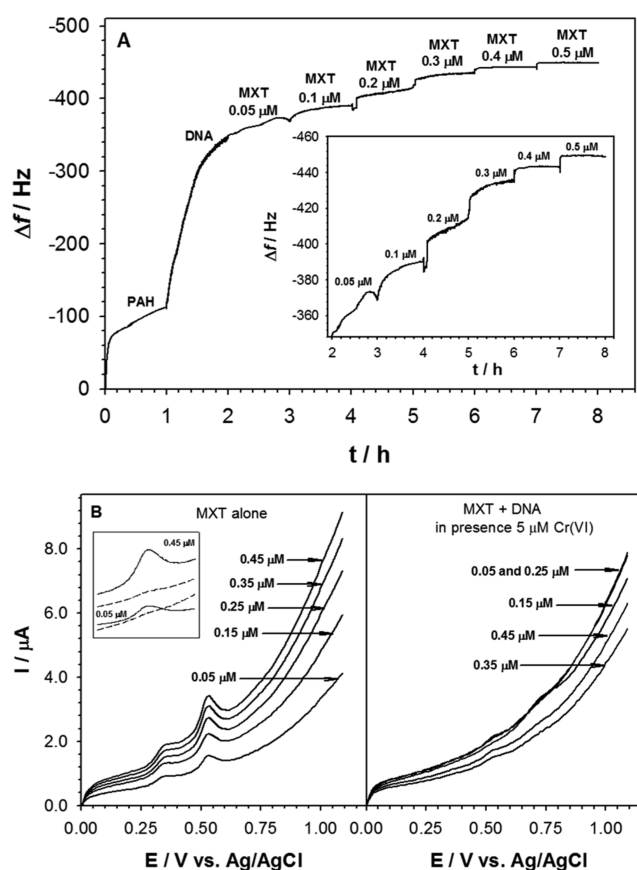


Figure 3. (A) EQCN frequency shifts recorded during subsequent steps of electrode surface modification obtained in 0.02 M PBS buffer (pH 7.4) in the presence of $5\text{ }\mu\text{M}$ Cr(VI). (B) Linear voltammograms of MXT obtained in the absence and presence of dsDNA and in the presence of $5\text{ }\mu\text{M}$ Cr(VI), for C_{MXT} ranging from 50 to 450 nM; conditions: $t = 23\text{ }^{\circ}\text{C}$; $\phi_{\text{GC}} = 3\text{ mm}$; $C_{\text{DNA}} = 2.6\text{ }\mu\text{M}$ bp, $\nu = 100\text{ mV/s}$; voltammograms were obtained 1 h after solution preparation.

concentration than the concentration of immobilized DNA), a decrease in the binding constant and an increase in the binding site size were observed. This effect is shown in Figure 4. The character of the changes in the plots shown in Figure 4 provides the basis to suggest a hypothesis that MXT actually protects the DNA from the damage by the Cr(VI) species. To verify this hypothesis, a second experimental approach has been used.

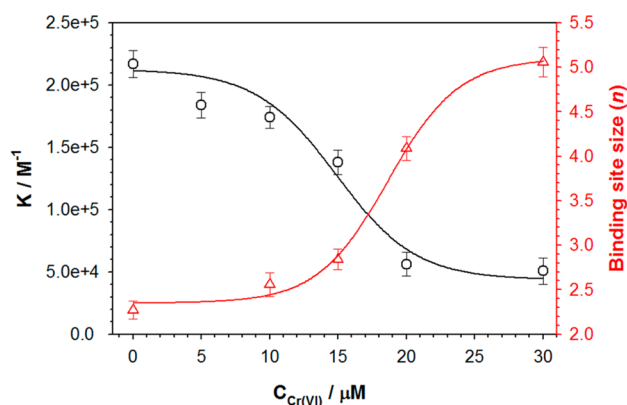


Figure 4. Dependencies of binding constant (K) and binding site size (n) for binding of MXT to dsDNA on concentration of Cr(VI) in solution, obtained from LSV and EQCN measurements.

Before the DNA interactions with MXT took place, the Au/PAH/DNA modified electrode had been immersed in the Cr(VI) solution for 15 min and after that the electrode had been carefully rinsed with distilled water and finally the cell was filled with a solution containing only MXT.

The obtained results confirm the above hypothesis. The immersion of a Au/PAH/DNA modified electrode in the solution containing only $1.5 \mu\text{M}$ Cr(VI) causes a decrease in the binding constant ($K = 0.94 \times 10^5 \text{ M}^{-1}$) by a factor of 3 and an increase in the binding site size ($n = 4.75$). The concentration of Cr(VI) higher than $5 \mu\text{M}$ leads to a complete damage of the DNA layer, rendering further interactions of DNA with MXT impossible. Typical responses of the nanobalance to increasing concentration of MXT are illustrated in Figure 5.

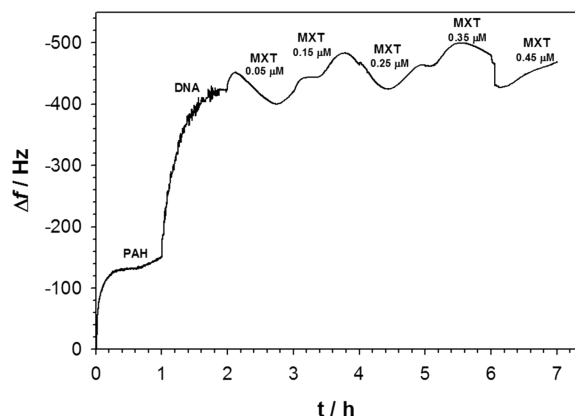


Figure 5. Frequency shifts recorded during subsequent steps of electrode surface modification obtained in 0.02 M PBS buffer (pH 7.4). Before the injection of MXT to the cell, the Au/PAH/DNA modified electrode was immersed in a $5 \mu\text{M}$ solution of Cr(VI) for 15 min.

Interaction of MXT with DNA in the Presence of Intermediate Valence States of Chromium: Cr(IV) and Cr(V). To expose a modified Au/PAH/DNA electrode to chromium species at the intermediate valence states, Cr(IV) and Cr(V), the electrode was immersed for 15 min in a Cr(VI) solution and polarized to $E = -200 \text{ mV}$. The mechanism of the Cr(VI) reduction is well described in the literature.^{72–74} The Cr(VI) reduction proceeds via a one-electron and one-proton

process to pentavalent chromium. In aqueous solutions of a neutral pH, Cr(V) rapidly disproportionates through a bimolecular mechanism, producing Cr(VI) and reactive Cr(IV) intermediates. However, at a more acidic pH, the disproportionation of this species is minimal and the decomposition is slow and attributed to the ligand oxidation. As is shown in Figure 6,

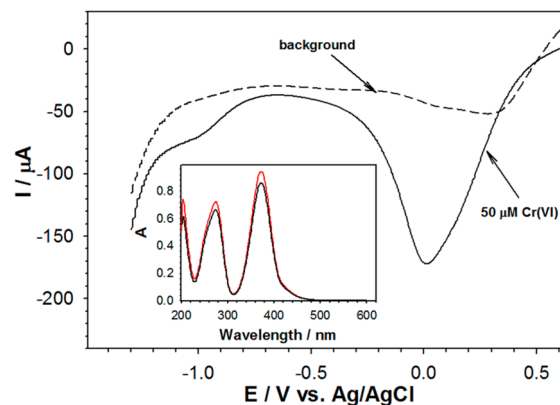


Figure 6. Cyclic voltammograms for a $50 \mu\text{M}$ Cr(VI) solution in 0.02 M PBS buffer (pH 7.4). Experimental conditions: $t = 23 \text{ }^\circ\text{C}$; $\phi_{\text{Au}} = 3 \text{ mm}$; solution degassed for 30 min with argon. Inset: UV-vis spectra for a 5 mM Cr(VI) solution obtained before (red line) and after (black line) application of a potential of -200 mV for 15 min (gold electrode) in 0.02 M PBS buffer (pH 7.4).

this procedure leads to the production of Cr(IV) and Cr(V) species. In particular, the absorbance decrease at 372 nm wavelength indicates that the intermediate valence states of chromium are really formed by applying -200 mV .

In the presence of chromium with the intermediate valence states, the biggest changes of binding parameters are observed. It is known that Cr(V) interacts with DNA.⁷⁵ This fact causes some binding sites to not be available for MXT. The mean values of the binding constant, K , and the binding-site size, n , determined from the Scatchard plot data, are $0.49 \times 10^5 \text{ M}^{-1}$ and 5.94, respectively. The procedure applied involved measurements using both the LSV and EQCN techniques. Because of the different electrode materials used in the LSV and EQCN measurements, different potentials were applied. The potential applied to the glassy carbon electrode had to be more negative by ca. 300 mV to ensure the efficient electrode reaction. Typical plots of frequency shifts and oxidation current changes during each treatment of the electrode surface are presented in Figure 7.

If the only reason for a decrease of the MXT–DNA binding constant and an increase in the binding site size were the interactions between Cr(V) and DNA, then an addition of a ligand complexing Cr(V) should minimize this effect. Such an experiment was done. Before the DNA interactions with MXT took place, the modified EQCN electrode (Au/PAH/DNA) was immersed in the mixture $5 \mu\text{M}$ Cr(VI) + $5 \mu\text{M}$ AA + $50 \mu\text{M}$ mannitol for 15 min. The original values of the binding constant, K , and the binding-site size, n , were recovered ($1.98 \times 10^5 \text{ M}^{-1}$ and 2.02, respectively).

To put these investigations into perspective, it has to be mentioned that reactive intermediates have been considered in the mechanisms of Cr(VI) genotoxicity. Among the three mechanisms proposed,^{76–79} the first considers highly reactive hydroxyl radicals and other radicals which are byproducts of the reduction of Cr(VI) to Cr(III). The second process includes

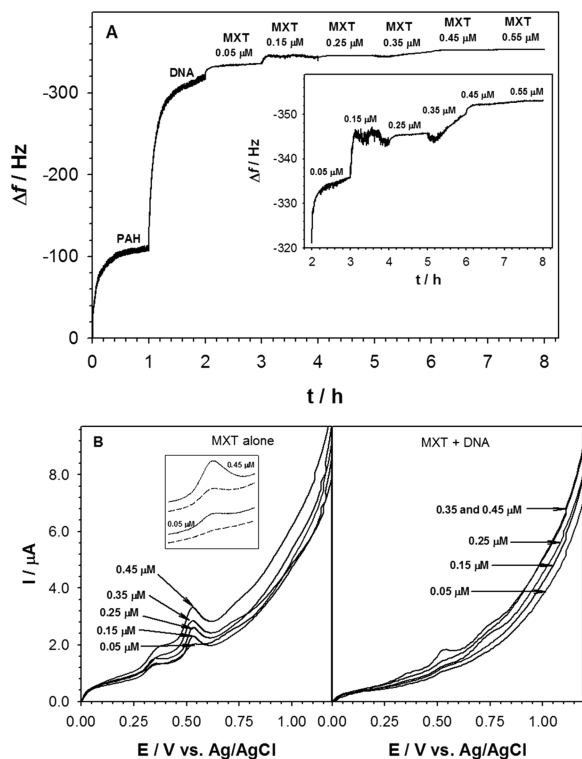


Figure 7. (A) EQCN frequency shifts upon each step of electrode surface modification obtained in 0.02 M PBS buffer (pH 7.4). The Au/PAH/DNA modified electrode was immersed for 15 min in 1.5 μM solution of Cr(VI) and polarized to -200 mV before placing in the cell with MXT solution. (B) Linear scan voltammograms of MXT obtained in the absence and presence of dsDNA; voltammograms were obtained 1 h after preparation of the mixture; before interactions with MXT, the glassy carbon electrode was polarized to -500 mV in a solution containing DNA + 1.5 μM Cr(VI) for 15 min and then MXT was added. Experimental conditions: $t = 23$ $^{\circ}\text{C}$; $\phi_{\text{GC}} = 3$ mm; C_{MXT} ranged from 50 to 450 nM; $C_{\text{DNA}} = 2.6$ μM bp, $\nu = 100$ mV/s.

direct binding of Cr(V), produced by the cellular reduction of Cr(VI), and Cr(IV) compounds to the DNA. The last mechanism attributed the genotoxicity to the binding of the end product of chromium reduction, the Cr(III) species, to the DNA.⁷⁷ The reaction of Cr(VI) with DNA creates a number of putative lesions in cellular systems including inter- and intrastrand cross-linked adducts, DNA–protein cross-links, DNA strand breaks, abasic sites, and oxidized nucleic acid bases.⁷⁶ Oxidative damage and the formation of oxidized lesions in DNA are considered one of the critical steps in the induction of carcinogenesis by Cr(VI). Oxidation of DNA can occur at the deoxyribose sugar, creating DNA strand breaks, or at the nucleic acid bases, creating oxidized base lesions.^{78,79}

Interaction of MXT with DNA in the Presence of Cr(III).

The data obtained in the presence of Cr(III) in the solution show that the Cr(III) species does not affect the intercalation of MXT into the dsDNA helix. The determined values of the binding constant, K , and the binding-site size, n , were found to be $2.33 \times 10^5 \text{ M}^{-1}$ and 2.03, respectively, which are very close to those obtained in the absence of chromium(III).

Fluorescence Spectra of the Interaction of MXT with DNA in the Presence of Cr(VI) and Cr(III). The interaction of MXT with DNA in the presence of Cr(VI) and Cr(III) in the same solution was also examined using the fluorescence titrations. The fluorescent excitation and emission spectra of

MXT as well as the effect of DNA concentration on the fluorescence emission spectra of MXT are illustrated in Figure 8A and B. MXT exhibited the excitation maximum at 596 nm

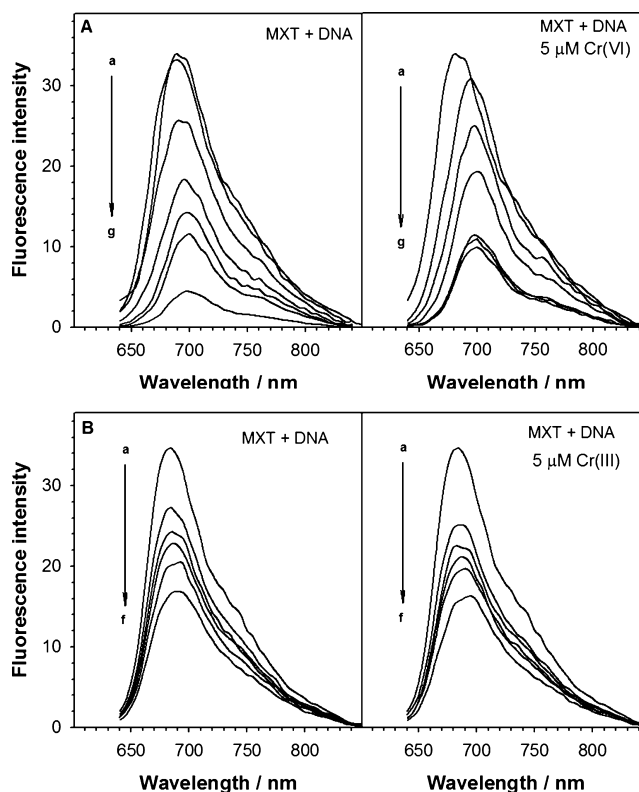


Figure 8. (A) MXT fluorescence emission quenching by titration with dsDNA in the absence and presence of a 5 μM Cr(VI) in 0.02 M PBS buffer (pH 7.4); $C_{\text{MXT}} = 2$ μM ; the excitation maximum $\lambda_{\text{ex}} = 596$ nm, C_{DNA} (μM): (a) 0, (b) 1.89, (c) 4.36, (d) 8.94, (e) 15, (f) 19.62, (g) 43.7; spectra were obtained 1 h after preparation of the mixture. (B) Same as in part A but in the absence and presence of a 5 μM Cr(III); C_{DNA} (μM): (a) 0, (b) 1.49, (c) 1.82, (d) 2.65, (e) 3.20, (f) 5.22; spectra were obtained 1 h after preparation of the mixture.

and the emission maximum at 688 nm. In both situations (in the presence of either Cr(VI) or Cr(III)), the fluorescence gradually decreased with increasing concentration of DNA in the solutions. This effect indicates that the MXT fluorescence was efficiently quenched upon binding to DNA. In addition to the changes in the fluorescence intensity, only in the presence of Cr(VI) in the solution, shifts in the wavelength were also observed. Such behavior indicates that Cr(VI) interacts with DNA and influences the DNA interactions with MXT.

The appropriate binding constants were estimated from the fluorescence measurements according to the Stern–Volmer equation:⁵²

$$\frac{F_0}{F} = 1 + K_{\text{SV}} C_{\text{DNA}} \quad (3)$$

where F_0 and F are the fluorescence intensities in the absence and presence of DNA, respectively, and K_{SV} is the Stern–Volmer quenching constant, which is a measure of the efficiency of DNA quenching. The titration data were used to construct plots of F_0/F versus C_{DNA} , which are presented in Figure 9A and 9B for the presence of Cr(VI) and Cr(III), respectively. K_{SV} values obtained from the slope of the lines are presented in Tables 1 and 2. Since the Stern–Volmer plots for

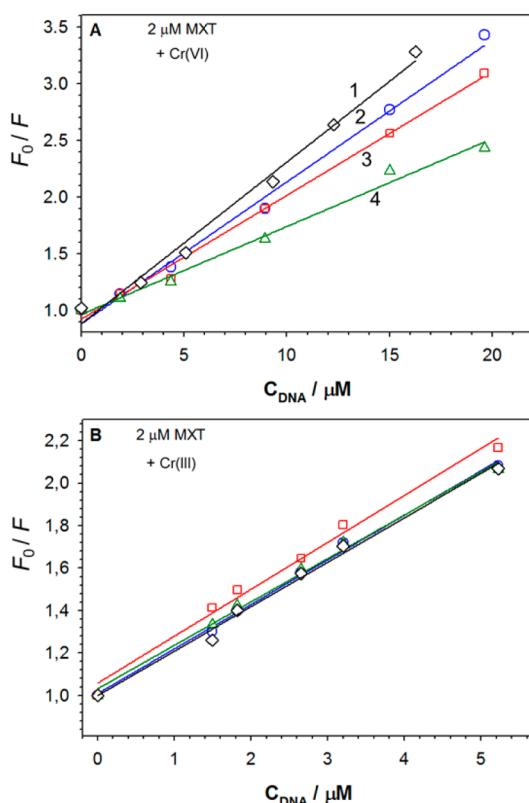


Figure 9. (A) Dependence of the Stern–Volmer quenching function F_0/F for MXT fluorescence on C_{DNA} for different concentrations of Cr(VI) in solution (μM): (1) 0, (2) 5, (3) 15, (4) 30. (B) Stern–Volmer quenching plot for different concentrations of Cr(III) in solution (μM): (1) 0, (2) 5, (3) 15, (4) 30; $C_{MXT} = 2 \mu\text{M}$.

both cases were linear, it means that only one type of quenching process occurs: either static or dynamic.⁸⁰ The research on an anthraquinone analogue of MXT showed that the fluorescence quenching was static.⁸¹ The fluorescence quenching is static, as evidenced by the high affinity constant, $K = (1.96 \pm 0.005) \times 10^5 \text{ M}^{-1}$, determined for MXT interaction with dsDNA. Further evidence has been obtained using the method of critical distance calculation,⁸² indicating that dynamic quenching is not likely to occur in the DNA–MXT system.

Mechanistic Aspects of Chromium Species Actions.

On the basis of the experiments performed, we can elucidate the effect of chromium species on the interactions of MXT with DNA. Mitoxantrone, as an intercalating compound, inserts to a DNA double helix preferentially between the nitrogen bases, guanine and cytosine, in a CpG base sequence, with the two positively charged chains extending outwardly to the negatively charged phosphate groups of the DNA backbone.^{10,12,23} In addition to that, various other MXT–DNA forms, including formaldehyde-activated minor and major groove adducts, methylation-enhanced minor groove adducts, and others, have been investigated.^{12,83} In the absence of a formaldehyde

Table 2. Binding Constants, K_b , and Binding Site Size, n , for Interactions between MXT and dsDNA in the Absence and Presence of Cr Species in 0.02 M PBS Buffer of pH 7.4

modified electrode treatment (Au/PAH/DNA)	$K_b \pm s(K_b) \text{ (M}^{-1}\text{)}$	$n \pm s(n)$
immersion in MXT solution	$(2.32 \pm 0.08) \times 10^5$	2.08 ± 0.15
immersion in mixture: MXT and 5 μM Cr(VI)	$(2.02 \pm 0.14) \times 10^5$	2.23 ± 0.10
immersion in 1.5 μM Cr(VI) solution before interactions between DNA and MXT	$(0.94 \pm 0.17) \times 10^5$	4.75 ± 0.25
immersion in 1.5 μM Cr(VI) solution with applied potential -200 mV before interactions between DNA and MXT	$(0.52 \pm 0.21) \times 10^5$	5.88 ± 0.20
immersion in mixture: 5 μM Cr(VI) + 5 μM AA + 50 μM mannitol before interactions between DNA and MXT	$(1.98 \pm 0.09) \times 10^5$	2.02 ± 0.23
immersion in mixture: MXT and 5 μM Cr(III)	$(2.33 \pm 0.09) \times 10^5$	2.03 ± 0.19

activation and/or methylation, the MXT intercalation remains the major path of the interaction of MXT with DNA. The effect of chromium species on MXT intercalation is complex. Our experiments and literature data indicate that the interaction of Cr(VI) with DNA induces, in the first step, the oxidation of guanine to oxoG but Cr(VI) does not form directly any high-affinity complexes with DNA due to the strong repulsions with the phosphate backbone of DNA. The chelation of lower valency chromium species, formed during the reduction of Cr(VI) , to the guanine N-7 could potentially influence the projection of MXT arms outward from the intercalated planar tricyclic chromophore, but our experiments with Cr(III) chelating to guanine N-7 in the major groove show that this is not the case. This means that the intercalation of MXT in DNA at the CpG site is from the minor groove. In this way, the Cr(III) chelation does not share any common binding sites with MXT. Thus, the presence of oxoG which reduces the stacking interactions of intercalated MXT and decreases the binding constant for the MXT–DNA complex becomes the major effect of Cr(VI) . The change in stacking interactions here is similar to that observed on replacing a guanine residue with oxoG in pure oligonucleotides.⁶⁵ The stacking interactions of MXT may even be decreased more if oxoG is further oxidized to spiroiminodihydantoin (Sp) or guanidinohydantoin (Gh),^{84–86} which is thermodynamically driven⁸⁷ but may be inhibited by DNA condensation due to MXT.

In order to explain why Cr(VI) induces a change in the MXT complexation with DNA, we consider the following arguments. First of all, Cr(VI) does not share a common binding site with MXT. In fact, Cr(VI) does not bind directly to DNA. The effect of Cr(VI) on MXT binding to DNA is primarily due to the modification of DNA by Cr(VI) , i.e., the oxidation of guanine to oxoG, which diminishes the MXT stacking interactions with nitrogen bases while intercalated in DNA. The stacking interactions are the major component of the MXT–DNA binding energy. The chelation of lower oxidation state chromium to guanine N-7 in the major groove might

Table 1. Binding Constant Values, $(\text{mol/L})^{-1}$, Obtained from Fluorescence Studies

	0 μM Cr(VI)	5 μM Cr(VI)	10 μM Cr(VI)	30 μM Cr(VI)
K_{SV}	$(1.96 \pm 0.005) \times 10^5$	$(1.25 \pm 0.015) \times 10^5$	$(1.09 \pm 0.026) \times 10^5$	$(0.77 \pm 0.018) \times 10^5$
	0 μM Cr(III)	5 μM Cr(III)	15 μM Cr(III)	30 μM Cr(III)
K_{SV}	$(2.09 \pm 0.09) \times 10^5$	$(2.10 \pm 0.07) \times 10^5$	$(2.21 \pm 0.12) \times 10^5$	$(2.05 \pm 0.13) \times 10^5$

potentially influence the projection of MXT side chains through the major groove, if MXT would intercalate from the major groove side, but it poses no problem for the intercalation of MXT from the minor groove. Since Cr(III) shows no effect on MXT affinity to DNA, we can conclude that it is the replacement of guanine with oxoG and the decrease in stacking interaction energy that is causing the overall decrease in the affinity of MXT to DNA in the presence of Cr(VI), observed experimentally.

The major structural modification of DNA due to the Cr(VI) is the oxidation of guanine residues to oxoG. Other indirect modifications may appear as a consequence of the increased ROS generation associated with the increased level of the oxidative stress caused by Cr(VI) species. On the other hand, no structural modifications of DNA due to Cr(III) species have been found except for reversible condensation observed at higher Cr(III) concentrations, confirming earlier studies.⁶⁴ The stability of DNA assessed by measuring changes in its melting temperature has been found to decrease with Cr(VI) concentration, in agreement with our^{37,38} and other studies.⁶⁵ However, in the presence of Cr(III), the DNA stability increases concomitant with the increase of DNA melting temperature. This behavior is consistent with other measurements of DNA stability.^{38,88}

In the absence of Cr species, mitoxantrone interactions with DNA result in DNA condensation.^{10,14} It follows from our experiments that the presence of Cr(III) species does not change this interaction and does not change the DNA conformation any further. However, in the presence of Cr(VI), additional conformation changes have been observed using circular dichroism (CD) measurements (not shown), most likely arising from the guanine oxidation by Cr(VI) and the presence of oxoG. As follows from the CD measurements, the DNA damage caused by Cr(VI) and conformation changes of DNA due to Cr(VI) are more extensive in the absence of MXT than in the presence of MXT.

The main course of chemotherapeutic action of MXT is the intercalation of MXT molecules into a DNA double helix, resulting in DNA condensation,^{10,15,17} which prevents DNA replication and inhibits RNA transcription.^{14,15} The MXT molecules intercalated into a DNA double helix are protected against oxidation by Cr(VI). This protection of MXT by double-stranded DNA has also been observed in Figure 3B and other electrochemical measurements.^{20,23} Hence, there is no damage to the main functional group of MXT, the anthracenedione aromatic triple ring. The observed slight reduction in MXT potency is due to the diminished affinity of MXT to DNA in the presence of Cr(VI) which is caused by the oxidation of DNA guanine to oxoG by Cr(VI). On the other hand, the Cr(III) interaction with guanine N-7 does not influence the intercalation and thus the potency of MXT.

The present experiments show clearly that the MXT affinity to DNA remains virtually unchanged in the presence of Cr(III). Along these lines, the effect of Cr(VI) should basically be even less noticeable than that of Cr(III) because of repulsions between CrO_4^{2-} and phosphate–deoxyribose chains of DNA. The observed weakening of the MXT–DNA binding in the presence of CrO_4^{2-} could not then be due to the Cr(VI) binding to DNA but rather to the oxidizing activity of the latter. In fact, CrO_4^{2-} species are able to oxidize the guanine residue of the GC base pairs in DNA, with the formation of oxoG. Since the MXT molecules bind to DNA by intercalation, predominantly at the CpG sites, it becomes clear that the

oxidizing reactivity of CrO_4^{2-} is responsible for the decrease in the binding strength of MXT to DNA.

CONCLUSIONS

We have investigated the affinity of a model drug, mitoxantrone, to DNA under varying conditions. We have found surprising differences between the action of two forms of chromium, Cr(III) species (binding strongly to DNA) and Cr(VI) species (forming no adducts with DNA), on MXT–DNA affinity. Cr(III) species, expected to interfere with MXT binding to DNA, have been found to have virtually no effect on MXT–DNA binding strength and MXT binding site size. On the other hand, Cr(VI) species, repelled electrostatically by DNA's negative charge, appeared to decrease the MXT–DNA binding strength and increase the binding site size from 2 to 4–6 bp, as determined by voltammetric, nanogravimetric, and fluorescence techniques, for DNA in solution, as well as for DNA immobilized on a polyamine-modified gold piezo-electrode. The latter arrangement has enabled controlling the electrode potential, being crucial for the selective delivery of Cr species with the given oxidation state, and direct observation of the binding and release processes.

AUTHOR INFORMATION

Corresponding Author

*E-mail: hepelmr@potdam.edu. Phone: +1.315.267.2267. Fax: +1.315.267.3170. Home Page: www2.potdam.edu/hepelmr.

Present Address

[§]Department of Chemistry, University of Warsaw, PL-02093 Warsaw, Poland.

Notes

The authors declare no competing financial interest.

ACKNOWLEDGMENTS

This work was supported by NSF CCLI Grant No. 0941-364.

ABBREVIATIONS

bp, base pair; CV, cyclic voltammetry; dsDNA, double-stranded DNA; EQCN, electrochemical quartz crystal nanogravimetry; CpG, cytosine–phosphate–guanine sequence; LSV, linear scan voltammetry; MXT, mitoxantrone; PAH, poly(allylamine hydrochloride)

REFERENCES

- (1) Thompson, C. M.; Fedorov, Y.; Brown, D. D.; Suh, M.; Proctor, D. M.; et al. *PLoS One* **2012**, *7* (8), e42720.
- (2) Velasco-Reynold, C.; Navarro-Alarcon, M.; Lopez-Ga De La Serrana, H.; Perez-Valero, V.; Lopez-Martinez, M. *Food Addit. Contam.* **2008**, *25*, 604–610.
- (3) Eastmond, D. A.; MacGregor, J. T.; Slesinski, R. S. *Crit. Rev. Toxicol.* **2008**, *38*, 173–190.
- (4) Qi, W.; Reiter, R. J.; Tan, D. X.; Manchester, L. C.; Siu, A. W.; Garcia, J. J. *J. Pineal Res.* **2000**, *29*, 54–61.
- (5) Shapiro, C. L.; Recht, A. N. *Engl. J. Med.* **2001**, *344*, 1997–2008.
- (6) Deley, M.C.L.; Suzan, F.; Cutulli, B.; Delalogue, S.; Shamsaldin, A.; Linassier, C.; Clisant, S.; Vathaire, F.d.; Fenaux, P.; Hill, C. J. *Clin. Oncol.* **2007**, *25*, 292–300.
- (7) Minotti, G.; Licata, S.; Saponiero, A.; Menna, P.; Calafiore, A. M.; Giammarco, G. D.; Liberi, G.; Animati, F.; Cipollone, A.; Manzini, S.; et al. *Chem. Res. Toxicol.* **2000**, *13*, 1336–1341.
- (8) Weiss, R. B. *Semin. Oncol.* **1992**, *19*, 670–686.
- (9) Lown, W.; Hanstock, C. C.; Bardley, R. D.; Scraba, D. C. *Mol. Pharmacol.* **1984**, *25*, 178–184.

- (10) Bartkowiak, J.; Kapuscinski, J.; Melamed, M. R.; Darzynkiewicz, Z. *Proc. Natl. Acad. Sci. U.S.A.* **1989**, *86*, 5151–5154.
- (11) Lown, W.; Morgan, A. R.; Yen, S.-F.; Wang, Y.-H.; Wilson, W. D. *Biochemistry* **1985**, *24*, 4028–4035.
- (12) Mazerski, J.; Martelli, S.; Borowski, E. *Acta Biochim. Pol.* **1998**, *45*, 1–11.
- (13) Capanico, G.; Zunino, F. In *Molecular Basis of Specificity in Nucleic Acid-Drug Interactions*; Pullman, B., Jortner, J., Eds.; Academic Publishers: Dordrecht, The Netherlands, 1990; pp 167–176.
- (14) Hajihassan, Z.; Rabbani-Chadegani, A. *J. Biomed. Sci.* **2009**, *16*, 31–36.
- (15) Chiang, S. Y.; Azizkhan, J. C.; Boorman, T. A. *Biochemistry* **1998**, *37*, 310–3115.
- (16) Fisher, G. R.; Patterson, L. H. *Cancer Chemother. Pharmacol.* **1992**, *30*, 451–458.
- (17) Huang, X.; Okafuji, M.; Traganos, F.; Luther, E.; Holden, E.; Darzynkiewicz, Z. *Cytometry, Part A* **2004**, *58*, 99–110.
- (18) Panousis, C.; Phillips, D. R. *Nucleic Acids Res.* **1994**, *22*, 1342–1345.
- (19) Bailly, C.; Henichart, J. P.; Colson, P.; Houssier, C. *J. Mol. Recognit.* **1992**, *15*, 155–171.
- (20) Li, N.; Ma, Y.; Yang, C.; Guo, L.; Yang, X. *Biophys. Chem.* **2005**, *116*, 199–205.
- (21) Brett, A. M. O.; Macedo, T. R. A.; Raimundo, D.; Marques, M. H.; Serrano, S. H. P. *Anal. Chim. Acta* **1999**, *385*, 401–408.
- (22) Mao, Y.; Hu, J.; Li, Q.; Xue, P. *Analyst* **2000**, *125*, 2299–2302.
- (23) Brett, A. M. O.; Macedo, T. R. A.; Raimundo, D.; Marques, M. H.; Serrano, S. H. P. *Biosens. Bioelectron.* **1998**, *13*, 861–867.
- (24) Erdem, A.; Özsoz, M. *Turk. J. Chem.* **2001**, *25*, 469–475.
- (25) Erdem, A.; Özsoz, M. *Electroanalysis* **2002**, *14*, 965–974.
- (26) Fojta, M. *Electroanalysis* **2002**, *14*, 1449–1463.
- (27) Wang, S.; Peng, T.; Yang, C. F. *Biophys. Chem.* **2003**, *104*, 239–248.
- (28) Nowicka, A.; Hafner, S.; Hepel, M. *ECS Trans.* **2009**, *19*, 1–13.
- (29) Hepel, M. Electrode-Solution Interface Studied with Electrochemical Quartz Crystal Nanobalance. In *Interfacial Electrochemistry. Theory, Experiment, and Applications*; Wieckowski, A., Ed.; M. Dekker: New York, 1999; pp 599–631.
- (30) Hepel, M.; Stobiecka, M. *Interactions of Herbicide Atrazine with DNA*; Nova Science Publishers: New York, 2010.
- (31) Nowicka, A. M.; Kowalczyk, A.; Stojek, Z.; Hepel, M. *Biophys. Chem.* **2010**, *146*, 42–53.
- (32) Hepel, M.; Stobiecka, M.; Nowicka, A. Nanogravimetric and voltammetric DNA-biosensors for screening of herbicides and pesticides. In *Biosensors and Environmental Health*; Preedy, V. R., Patel, V., Eds.; CRC Press: Boca Raton, FL, 2012; pp 230–255.
- (33) Stobiecka, M.; Cieřla, J. M.; Janowska, B.; Tudek, B.; Radecka, H. *Sensors* **2007**, *7*, 1462–1479.
- (34) Stobiecka, M.; Hepel, M. *Biomaterials* **2011**, *32*, 3312–3321.
- (35) Hepel, M.; Stobiecka, M. Novel DNA-Hybridization Biosensors for Studies of Atrazine Interactions with DNA. In *Adv. Environ. Res.*; Daniels, J. A., Ed.; Nova Sci. Publ.: New York, 2011; Vol. 6, pp 253–298.
- (36) Hepel, M.; Stobiecka, M. Detection of Oxidative Stress Biomarkers Using Functional Gold Nanoparticles. In *Fine Particles in Medicine and Pharmacy*; Matijevic, E., Ed.; Springer Sci Publ.: New York, 2012; pp 241–281.
- (37) Stobiecka, M.; Prance, A.; Coopersmith, K.; Hepel, M. Antioxidant effectiveness in preventing paraquat-mediated oxidative DNA damage in the presence of H₂O₂. In *Oxidative Stress: Diagnostics, Prevention and Therapy*; Andreescu, S., Hepel, M., Eds.; Oxford University Press: Oxford, U.K., 2011; Vol. 1083, pp 211–233.
- (38) Hepel, M.; Stobiecka, M.; Peachey, J.; Miller, J. *Mutat. Res.* **2012**, *735*, 1–11.
- (39) Fan, C. H.; Plaxco, K. W.; Heeger, A. J. *Trends Biotechnol.* **2005**, *23*, 186–192.
- (40) Drummond, T. G.; Hill, M. G.; Barton, J. K. *Nat. Biotechnol.* **2003**, *21*, 1192–1199.
- (41) Zhang, J.; Lao, R.; Song, S.; Yan, Z.; Fan, C. *Anal. Chem.* **2008**, *80*, 9029–9033.
- (42) Su, X. *Biochem. Biophys. Res. Commun.* **2002**, *290*, 962–966.
- (43) Chang, Z.; Chen, M.; Fan, H.; Zhao, K.; Zhuang, S.; He, P.; Fang, Y. *Electrochim. Acta* **2008**, *53*, 2939–2945.
- (44) Mir, M.; Alvarez, M.; Azzaroni, O.; Tiefenauer, L.; Knoll, W. *Anal. Chem.* **2008**, *80*, 6554–6559.
- (45) Pang, D. W.; Abruna, H. D. *Anal. Chem.* **1998**, *70*, 3162–3169.
- (46) Ferencova, A.; Adamovski, M.; Grundler, P.; Zima, J.; Barek, J.; Mattusch, J.; Wennrich, R.; Labuda, J. *Bioelectrochemistry* **2007**, *71*, 33–37.
- (47) Galandova, J.; Ovadekova, R.; Ferencova, A.; Labuda, J. *Anal. Bioanal. Chem.* **2009**, *394*, 855–861.
- (48) Hianik, T. *DNA/RNA aptamers - novel recognition structures in biosensing*; Elsevier: Amsterdam, The Netherlands, 2007.
- (49) Hianik, T.; Ostatna, V.; Sonlajtnerova, M.; Grman, I. *Bioelectrochemistry* **2007**, *70*, 127–133.
- (50) Lim, I. I. S.; Chandrachud, U.; Wang, L.; Gal, S.; Zhong, C. J. *Anal. Chem.* **2008**, *80*, 6038–6044.
- (51) Mirkin, C. A.; Letzinger, R. L.; Mucic, R. C.; Storhoff, J. J. *Nature* **1996**, *382*, 607–609.
- (52) Pyle, A. M.; Rehmann, J. P.; Meshoyrer, R.; Kumar, C. V.; Turro, N. J.; Barton, J. K. *J. Am. Chem. Soc.* **1989**, *111*, 3051–3058.
- (53) Vacek, J.; Mozga, T.; Cahova, K.; Pivonkova, H.; Fojta, M. *Electroanalysis* **2007**, *19*, 2093–2102.
- (54) Mertz, W. *J. Nutr.* **1993**, *123*, 626–633.
- (55) Liu, S.; Dixon, K. *Environ. Mol. Mutagen.* **1996**, *28*, 71–79.
- (56) O'Brien, T. J.; Ceryak, S.; Patierno, S. R. *Mutat. Res.* **2003**, *533*, 3–36.
- (57) Quievryn, G.; Peterson, E.; Messer, J.; Zhitkovich, A. *Biochemistry* **2003**, *42*, 1062–1070.
- (58) Feng, Z.; Hu, W.; Rom, W. N.; Costa, M.; Tang, M. S. *Carcinogenesis* **2003**, *24*, 771–778.
- (59) Langard, S. *Am. J. Ind. Med.* **1990**, *17*, 189–215.
- (60) Vincent, J. B. *Proc. Nutr. Soc.* **2004**, *63*, 41–47.
- (61) Katz, S. A.; Salem, H. *J. Appl. Toxicol.* **1993**, *13*, 217–224.
- (62) Stearns, D. M.; Wise, J. P.; Patierno, S. R.; Wetterhahn, K. E. *FASEB J.* **1995**, *9*, 1643–1649.
- (63) Dayan, A. D.; Paine, A. J. *Hum. Exp. Toxicol.* **2001**, *20*, 439–451.
- (64) Arakawa, H.; Ahmad, R.; Naoui, M.; Tajmir-Riahi, D. A. *J. Biol. Chem.* **2000**, *275*, 10150–10153.
- (65) Singh, S. K.; Szulik, M. W.; Ganguly, M.; Khutsishvili, I.; Stone, M. P.; Marky, L. A.; Gold, B. *Nucleic Acids Res.* **2011**, *1*–13.
- (66) McFadyen, W. D.; Sotirellis, N.; Denny, W. A.; Wakelin, P. G. *Biochem. Biophys. Acta* **1990**, *1048*, 50–58.
- (67) Sauerbrey, G. *Z. Phys.* **1959**, *155*, 206–222.
- (68) Trasatti, S.; Petrii, O. A. *Pure Appl. Chem.* **1991**, *63*, 711–734.
- (69) McGhee, J. D.; von Hippel, P. H. *J. Mol. Biol.* **1974**, *86*, 469–489.
- (70) Villar, J. C. C.; Garcia, A. C.; Blanco, P. T. *Talanta* **1993**, *40*, 325–331.
- (71) Ibrahim, M. S. *Anal. Chim. Acta* **2001**, *443*, 63–72.
- (72) Gould, E. S. *Coord. Chem. Rev.* **1994**, *135/136*, 651–684.
- (73) Sugden, K. D.; Wetterhahn, K. E. *Inorg. Chem.* **1996**, *35*, 651–657.
- (74) Welch, C. M.; Nekrassova, O.; Compton, R. G. *Talanta* **2005**, *65*, 74–80.
- (75) Stearns, D. M.; Courtney, K. D.; Giangrande, P. H.; Phieffer, L. S.; Wetterhahn, K. E. *Environ. Health Perspect.* **1994**, *102*, 21–25.
- (76) Miller, C. A.; Costa, M. *Mol. Carcinog.* **1988**, *1*, 125–133.
- (77) Cohen, M. D.; Kargacin, B.; Klein, C. B.; Costa, M. *Crit. Rev. Toxicol.* **1993**, *23*, 255–281.
- (78) Pratviel, G.; Bernadou, J.; Meunier, B. *Angew. Chem., Int. Ed.* **1995**, *34*, 746–769.
- (79) Burrows, C. J.; Muller, J. G. *Chem. Rev.* **1998**, *98*, 1109–1151.
- (80) Lakowicz, J. R. *Principles of Fluorescence Spectroscopy*; Kluwer Academic: New York, 2006.

- (81) Zhong, W.; Yu, J. S.; Huang, W. L.; Ni, K. Y.; Liang, Y. Q. *Biopolymers* **2001**, 62, 315–323.
- (82) Stobiecka, M.; Hepel, M. *Phys. Chem. Chem. Phys.* **2011**, 13, 1131–1139.
- (83) Parker, B. S.; Buley, T.; Evison, B. J.; Cutts, S. M.; Neumann, G. M.; Iskander, M. N.; Phillips, D. R. *J. Biol. Chem.* **2004**, 279, 18814–18823.
- (84) Luo, W.; Muller, J. G.; Rachlin, E. M.; Burrows, C. J. *Org. Lett.* **2000**, 2, 613–616.
- (85) Luo, W.; MJ., Burrows, C. J. *Org. Lett.* **2001**, 3, 2801–2804.
- (86) Slade, P. G.; Hailer, M. K.; Martin, B. D.; Sugden, K. D. *Chem. Res. Toxicol.* **2005**, 18, 1140–1149.
- (87) Steenken, S.; Jovanovic, S. V.; Bietti, M.; Bernhard, K. *J. Am. Chem. Soc.* **2000**, 122, 2372–2374.
- (88) Stobiecka, M.; Molinero, A. A.; Chalupa, A.; Hepel, M. *Anal. Chem.* **2012**, 84, 4970–4978.